Supplementary Information

Application of neutral d^{10} coinage metal complexes with an anionic bidentate ligand in delayed fluorescence-type organic light-emitting diodes

Masahisa Osawa,*[,a] Isao Kawata,[a,c] Ryuji Ishii,[b] Satoshi Igawa,[a,b] Masashi Hashimoto,[a,b] and Mikio Hoshino[a]

[a]*Luminescent Materials Laboratory, RIKEN, Hirosawa 2-1, Wako-Shi, 351-0198, Japan.*
[b]*Device Technology Development Headquartersc, Ohta-ku, Tokyo 146-8501, Japan.*
[c]*Analysis Technology Center, Canon Incorporated, Ohta-ku, Tokyo 146-8501, Japan.*

Contents

Experimental Details

1. Synthetic Details

Materials. 1,2-bis(diphenylphosphino)benzene (PP) and sodium hydride (60%, dispersion in paraffine liquid) were obtained from TCI. Co., Ltd. Silver bromide and poly(9-vinylcarbazole) (PVK) was purchased from Sigma-Aldrich. PEDOT: PSS (CLEVIOS^{TM} P VP CH 8000) was obtained from Heraeus Clevios GmbH. 4,4'-bis(9-carbazolyl)-2,2'-dimethyl-biphenyl (CDBP), Di-[4-(N,N-ditolyl-amino)-phenyl]cyclohexane (TAPC), 1,3-bis(carbazol-9-yl)benzene (mCP), and tris(2,4,6-trimethyl-3-(pyridine-3-yl)phenyl)borane (3TPYMB) were purchased from Lumitec Corp. xylene (EL grade) was obtained from Kanto Chemical Co., Inc. 2-Diphenylphosphinobenzenethiol (PSH),[1] $[Cu(\mu\text{-}Br)(PP)]_2$,[2] and $Au(PPh_3)Cl$[3] were prepared according to the literature.

[Cu(PP)(PS)] (1). A tetrahydrofuran (10 ml) solution of 2-diphenylphosphinobenzenethiol, sodium salt (PSNa) was prepared from sodium hydride (10 mg, 0.42 mmol) and 2-diphenylphosphinobenzenethiol (120 mg, 0.41 mmol). The solution of PSNa was added to a THF (20 ml) solution of $[Cu(\mu\text{-}Br)(PP)]_2$ (230 mg, 0.20 mmol) and was stirred for 2 h at room temperature. After filtration of the reaction mixture, the solvent was removed in vacuo to give a pale yellow powder. The residue was purified by recrystallization from CH_2Cl_2 / acetone to give yellow crystals Cu(PP)(PS) (**1**) (223 mg, 73%). ^{1}H NMR (400 MHz, CD_2Cl_2, 220 K): δ 6.65 (m, 4H), 6.70 (t, 1H, *J* = 7.4 Hz), 6.82 (t, 4H, *J* = 7.6 Hz), 6.93 (t, 4H, *J* = 7.5 Hz), 7.10 (m, 7H), 7.29 (m, 16H), 7.47 (m, 4H), 7.55 (m, 1H); ^{31}P {^{1}H }NMR (162 MHz, CD_2Cl_2, 220 K) δ 10.1 (s, br), 2.67 (s, br). Anal. calcd. for $C_{48}H_{38}CuP_3S$ (%): C, 71.76; H, 4.77. Found: C, 71.55; H, 5.03.

$[Ag(\mu\text{-}Br)(PP)]_2$. A round battle flask was charged with AgBr (90mg, 0.48 mmol), PP (200 mg, 0.45 mmol) in 30 ml of CH_2Cl_2. After the mixture was stirred for 12 h at room temperature in the dark. Then, the reaction mixture was filtrated, and the solvent was removed in vacuo to give a white powder. A colorless crystalline sample was obtained by diffusion of ether on the surface of the CH_2Cl_2 solution dissolving $[Ag(\mu\text{-}Br)(PP)]_2$.. Yield: 251 mg, 88%. ^{1}H NMR (400 MHz, CD_2Cl_2, 300 K) δ 7.54 (m, 4H), 7.25 (m, 20H); ^{31}P {^{1}H }NMR (162 MHz, CD_2Cl_2, 300 K) δ -4.26 (br). Anal. Calcd for $C_{60}H_{48}Ag_2Br_2P_4$: C, 56.81; H, 3.81. Found C, 57.02; H, 3.59.

[Ag(PP)(PS)] (2). This compound was prepared similarly to Cu(PP)(PS) (**1**), except that the $[Ag(\mu\text{-}Br)(PP)]_2$ (241 mg, 0.19 mmol) was used instead of $[Cu(\mu\text{-}Br)(PP)]_2$. Analytically pure material was obtained by recrystallization from THF. Yield: 184 mg, 57%. ^{1}H NMR (400 MHz, CD_2Cl_2, 300 K): δ 6.70 (t, 1H, *J* = 7.7 Hz), 6.94 (m, 2H), 7.17 (m, 12H), 7.31 (m, 22H), 7.70 (t,

1H, J = 7.0 Hz); ^{31}P {^{1}H }NMR (162 MHz, $CDCl_3$, 220 K) δ 3.53 (dt, $^{1}J(^{31}P\text{-}^{107}Ag)$ = 288 Hz, $^{1}J(^{31}P\text{-}^{109}Ag)$ = 333 Hz, $^{2}J(^{31}P\text{-}^{31}P)$ = 34 Hz), -7.01 (dd, $^{1}J(^{31}P\text{-}^{107}Ag)$ = 223 Hz, $^{1}J(^{31}P\text{-}^{109}Ag)$ = 258 Hz, $^{2}J(^{31}P\text{-}^{31}P)$ = 34 Hz). Anal. calcd. for $C_{48}H_{38}AgP_3S$ (%): C, 68.01; H, 4.52. Found: C, 67.80; H, 4.34.

[Au(PP)(PS)] (3). $Au(PPh_3)Cl$ (100 mg, 0.20 mmol) and PSH (60 mg, 0.20 mmol) were stirred for 10 min in a mixed solvent (5 ml of THF and 5 ml of ether). The color of solution immediately turned from colorlessness to yellow. A solution (4 ml of THF and 8 ml of ether) of PP (100 mg, 0.20 mmol) was added to the yellow reaction mixture slowly and then yellow microcrystals of Au(PP)(PS) **3** were deposited instantly. The yellow crystals of **3** were isolated by filtration. Yield: 99 mg, 53%. ^{1}H NMR (400 MHz, CD_2Cl_2, 300 K): δ 6.70 (t, 1H, J = 7.7 Hz), 6.92 (t, 1H, J = 7.7 Hz), 7.00 (t, 1H, J = 7.4 Hz), 7.07 (t, 4H, J = 7.0 Hz), 7.30 (m, 28H), 7.56 (m, 2H), 7.70 (t, 1H, J = 7.0 Hz); ^{31}P {^{1}H }NMR (162 MHz, CD_2Cl_2, 300 K) δ 26.3 (t, $J(^{31}P\text{-}^{31}P)$ = 83.9 Hz), 18.3 (d, $J(^{31}P\text{-}^{31}P)$ = 83.9 Hz. Anal. calcd. for $C_{48}H_{38}AuP_3S$ (%): C, 61.54; H, 4.09. Found: C, 61.36; H, 4.21.

2. NMR Experiments

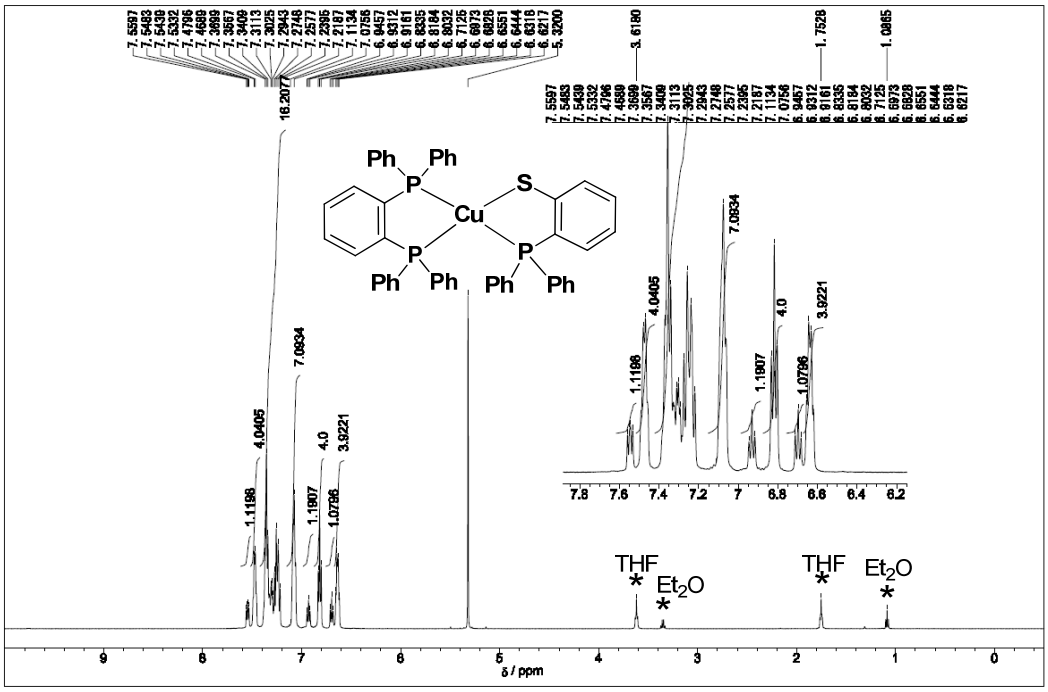

Fig. S1 ^{1}H NMR spectrum of **1** in CD_2Cl_2 at 220 K.

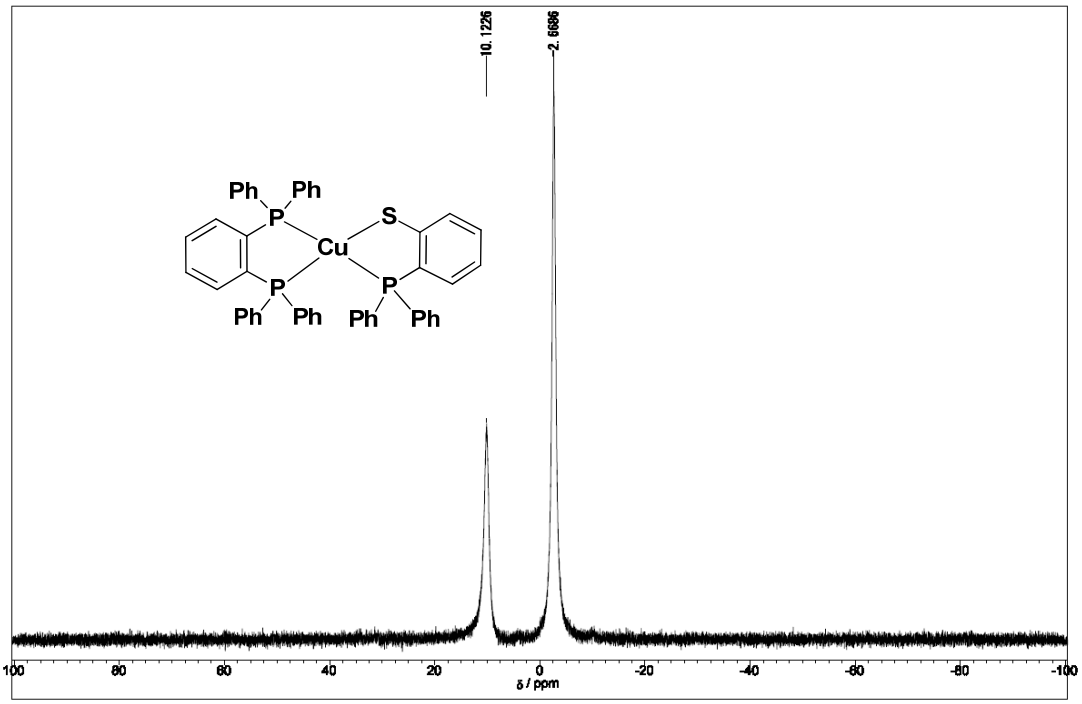

Fig. S2 ^{31}P $\{^{1}H\}$ NMR spectrum of **1** in CD_2Cl_2 at 220 K.

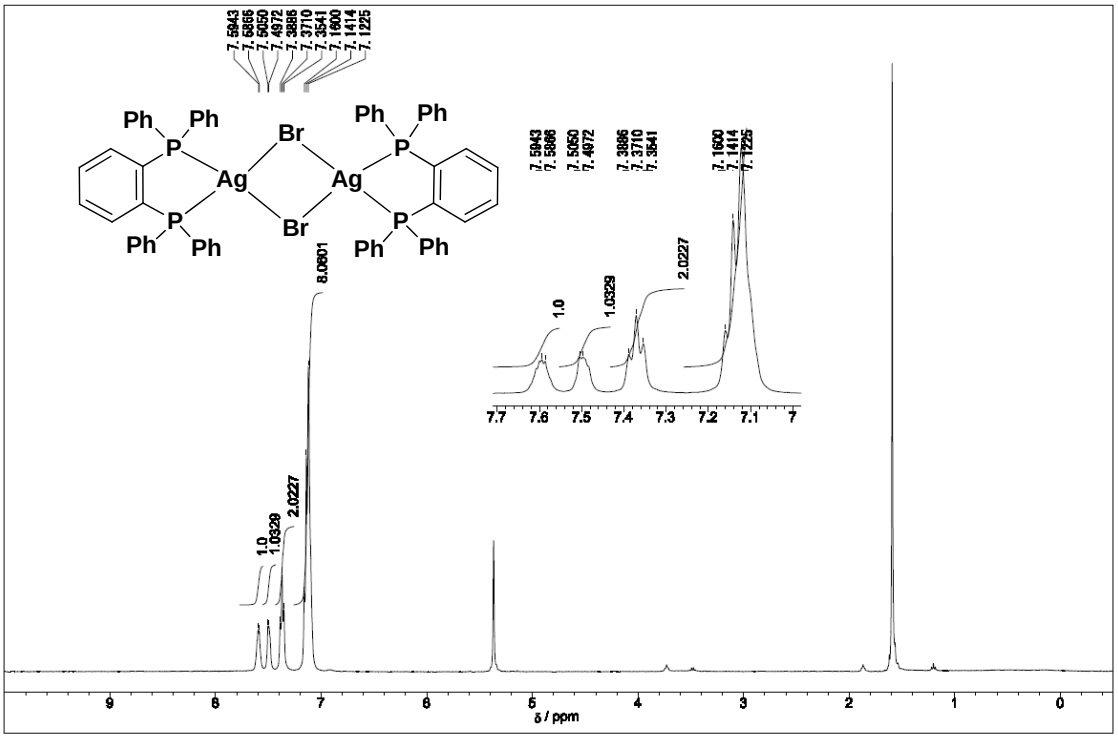

Fig. S3 ^{1}H NMR spectrum of $[Ag(\mu\text{-}Br)(PP)]_2$ in CD_2Cl_2 at 300 K.

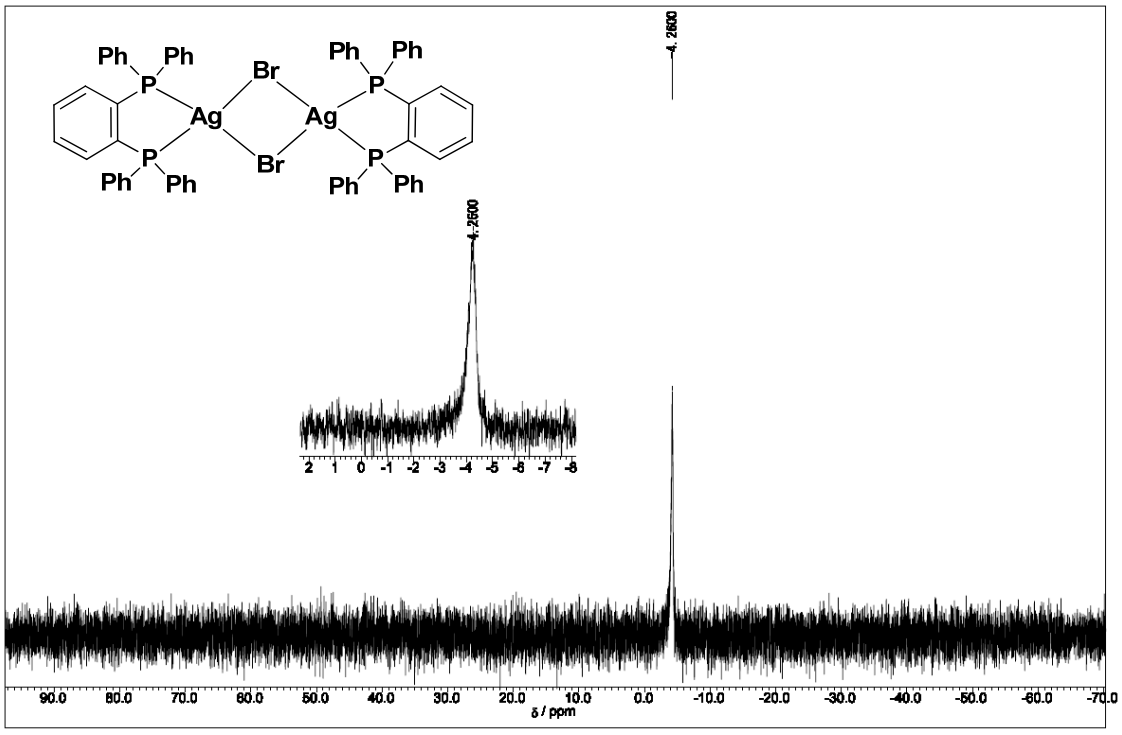

Fig. S4 ^{31}P $\{^{1}H\}$ NMR spectrum of $[Ag(\mu\text{-}Br)(PP)]_2$ in CD_2Cl_2 at 300 K.

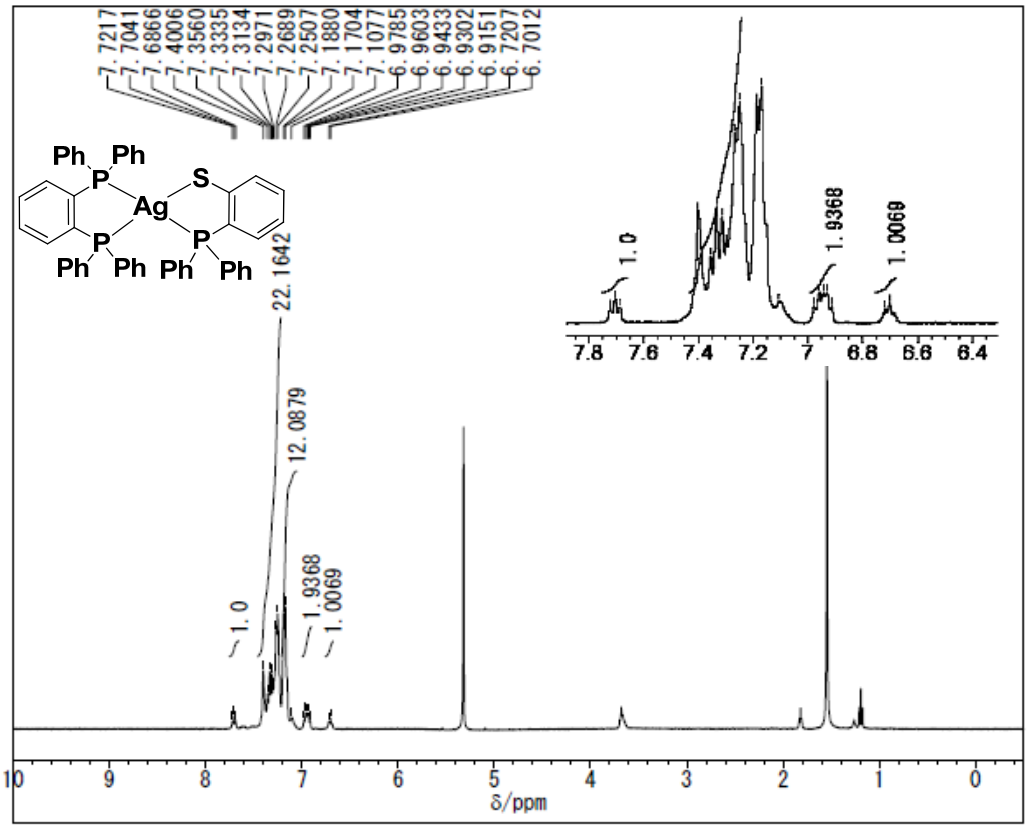

Fig. S5 ^{1}H NMR spectrum of **2** in $CDCl_3$ at 300 K.

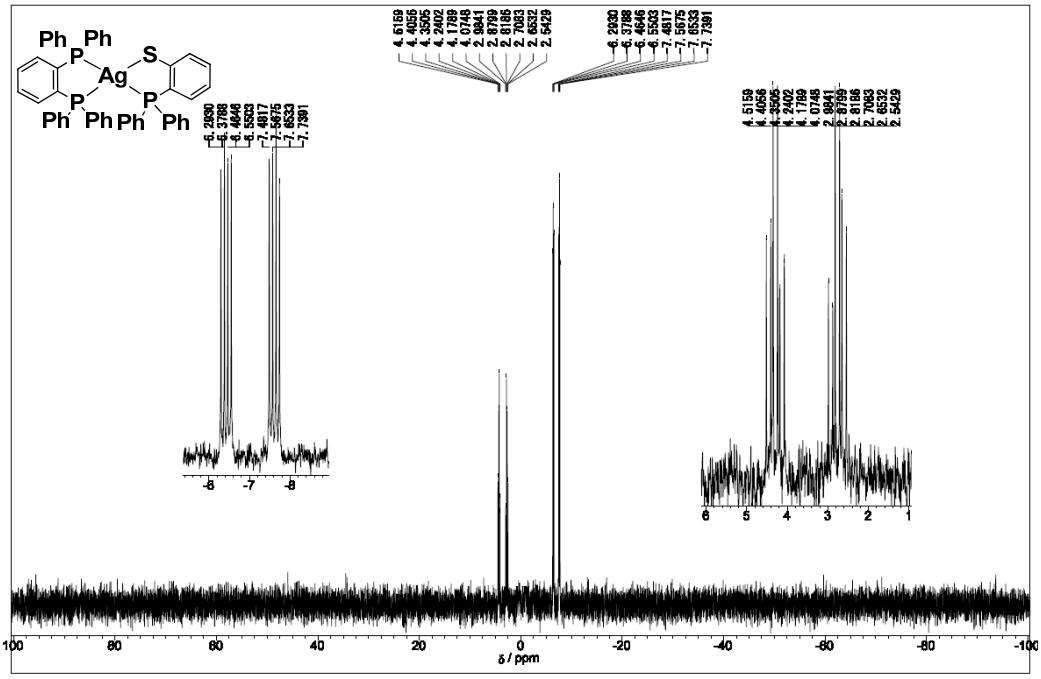

Fig. S6 ^{31}P $\{^{1}H\}$ NMR spectrum of **2** in $CDCl_3$ at 220 K.

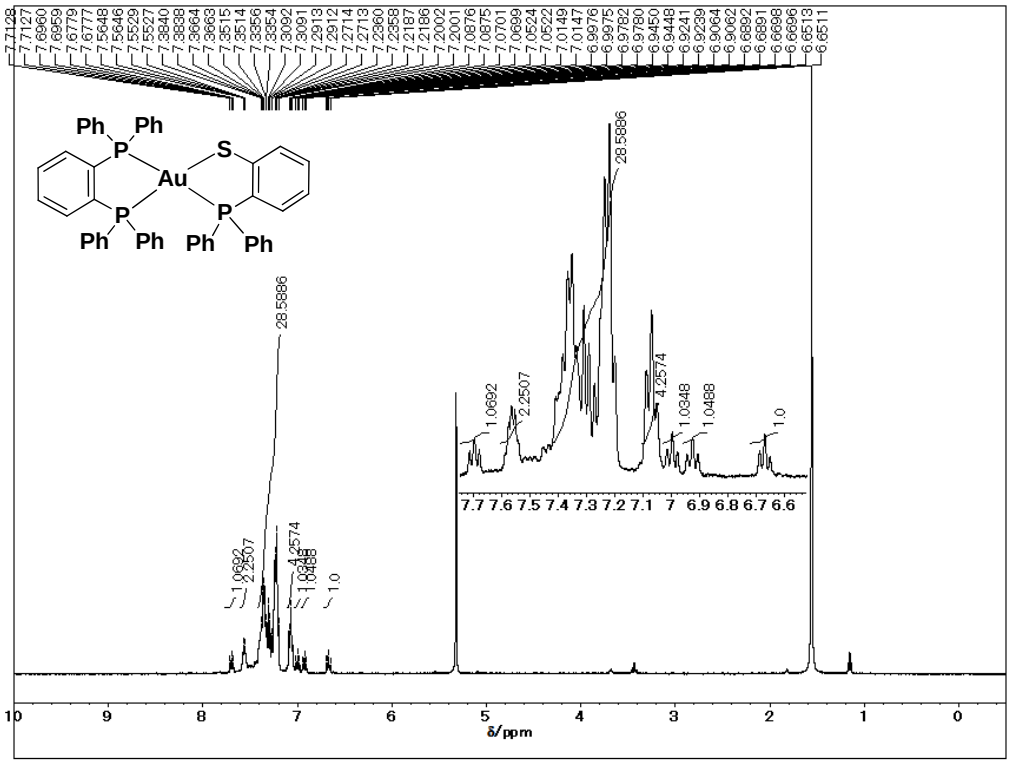

Fig. S7 ^{1}H NMR spectrum of **1** in CD_2Cl_2 at 300 K.

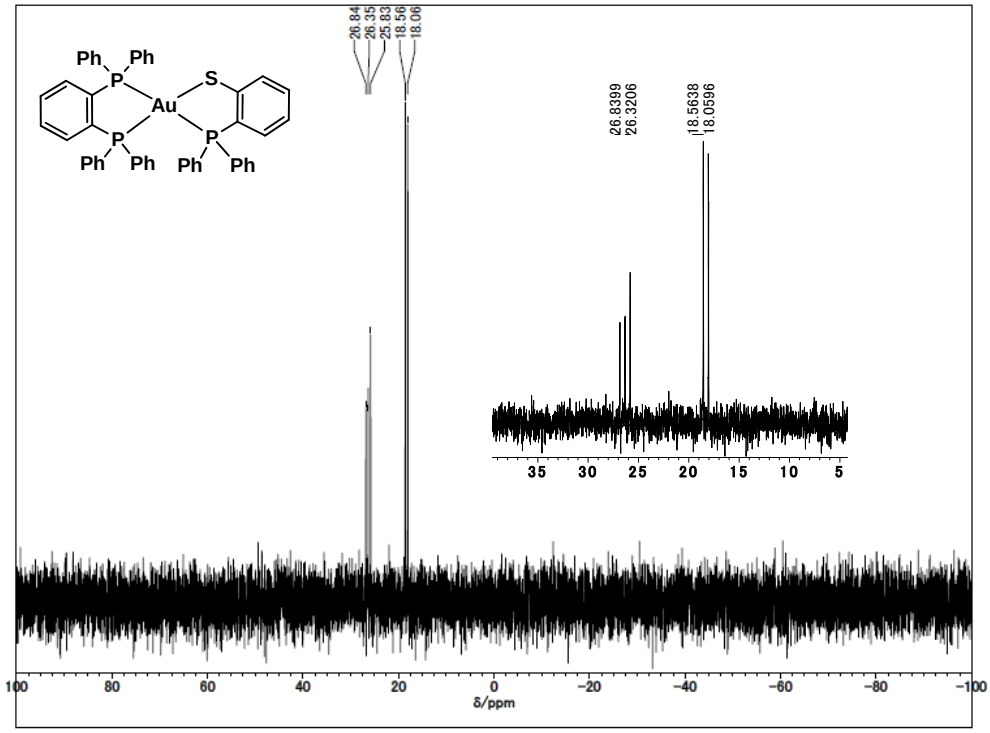

Fig. S8 ^{31}P {^{1}H} NMR spectrum of **1** in CD_2Cl_2 at 300 K.

3. Crystal Structure Determination

Table S1 Crystallographic data for **1**−**3**

	1	**2**	**3**
formula	$C_{48}H_{38}BCuP_3S$	$C_{48}H_{38}AgP_3S$	$C_{48}H_{38}AuP_3S$
formula weight	803.29	847.62	936.72
cryst syst	triclinic	triclinic	triclinic
space group	$P\bar{1}$	$P\bar{1}$	$P\bar{1}$
a / Å	10.9321 (11)	10.8301 (6)	10.8554 (18)
b / Å	17.2890 (14)	12.0774 (6)	12.0178 (18)
c / Å	21.859 (2)	15.8880 (9)	15.617 (2)
α / deg	74.282 (5)	72.281 (2)	73.052 (6)
β / deg	80.472 (5)	88.762 (2)	88.148 (9)
γ / deg	82.288 (6)	81.290 (3)	80.401 (7)
V / Å^3	3904.8 (6)	1956.06 (18)	1921.3 (5)
Z	4	2	2
d_{calcd} / g cm^{-3}	1.366	1.439	1.619
T / K	90.0(1)	90.0(1)	90.0(1)
radiation	Mo Kα	Mo Kα	Mo Kα
	(λ = 0.71073 Å)	(λ = 0.71073 Å)	(λ = 0.71073 Å)
μ / cm^{-1}	0.770	0.675	4.043
diffractometer	Rigaku AFC-8	Rigaku AFC-8	Rigaku AFC-8
max 2θ / deg	60	55	60
reflns collcd	102460	29243	20603
indep reflns	22754	19205	11101
	(*R*int = 0.079)	(*R*int = 0.056)	(*R*int = 0.040)
no. of param refined	955	479	479
R1, *wR2* ($I > 2\sigma I$)	0.0723, 0.1604	0.0433, 0.1031	0.0491, 0.0832
S	1.098	1.050	1.076

4. Theoretical Studies

Table S2 Calculated energy differences between sublevels (M1, M2, and M3) in T_1 states for **1** – **3**

energy level [a]	**1**	**2**	**3**
M1	20769.9	19828.8	19900.4
M2	20760.9	19828.8	19900.6
M3	20760.9	19828.8	19904.3

[a] cm^{-1}

Table S3 Compositions of hole and electron in S_1 of **1**. (X-ray crystal structure)

	percentage composition (%) [a]		
	hole	electron	differences
Cu	5.27	0.65	4.62
S	59.4	0.08	59.3
P	3.82	1.48	2.34
P	2.52	4.37	-1.85
P	0.19	0.27	-0.08
others	27.1	93.1	-66.0

[a] In the molecular orbitals, the atomic component is evaluated by the sum of the square of the LCAO coeffiients which belong to the corresponding atom; see experimental section in detail.

Table S4 Compositions of hole and electron in T_1 of **1**. (X-ray crystal structure)

	percentage composition (%) [a]		
	hole	electron	differences
Cu	5.44	0.72	4.72
S	58.5	0.09	58.4
P	4.04	1.49	2.55
P	2.77	4.43	-1.66
P	0.21	0.29	-0.08
others	29.1	93.0	-66.0

[a] In the molecular orbitals, the atomic component is evaluated by the sum of the square of the LCAO coeffiients which belong to the corresponding atom; see experimental section in detail.

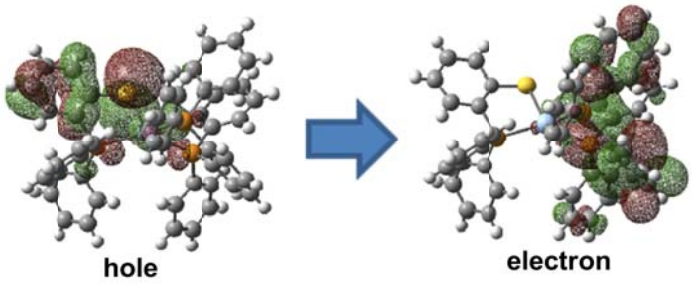

Fig. S9 NTO pairs for the lowest singlet excited state of **2** in X-ray crystal structure.

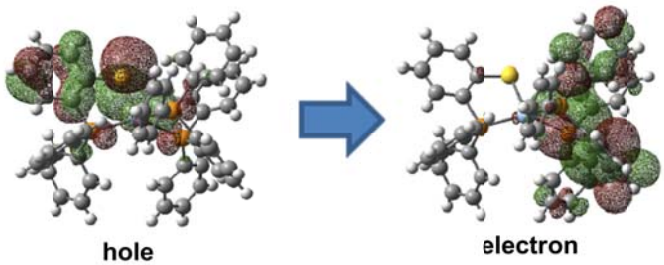

Fig. S10 NTO pairs for the lowest triplet excited state of **2** in X-ray crystal structure.

Table S5 Compositions of hole and electron in S_1 of **2**. (X-ray crystal structure)

	percentage composition (%) [a]		
	hole	electron	differences
Ag	2.47	0.52	1.95
S	62.4	0.04	62.4
P	1.87	3.87	-2.00
P	0.93	1.01	-0.08
P	1.27	0.27	1.00
others	31.0	94.3	-63.3

[a] In the molecular orbitals, the atomic component is evaluated by the sum of the square of the LCAO coeffiients which belong to the corresponding atom; see experimental section in detail.

Table S6 Compositions of hole and electron in T_1 of **2**. (X-ray crystal structure)

	percentage composition (%) [a]		
	hole	electron	differences
Cu	2.55	055	2.00
S	61.8	0.06	61.2
P	2.05	3.88	-1.83
P	1.14	1.00	0.14
P	1.27	0.30	0.97
others	31.2	94.2	-63.0

[a] In the molecular orbitals, the atomic component is evaluated by the sum of the square of the LCAO coeffiients which belong to the corresponding atom; see experimental section in detail.

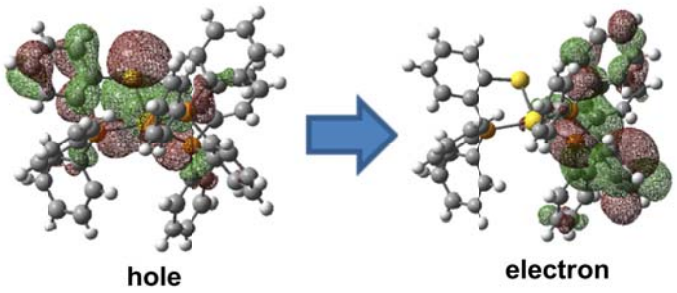

Fig. S11 NTO pairs for the lowest singlet excited state of **3** in X-ray crystal structure.

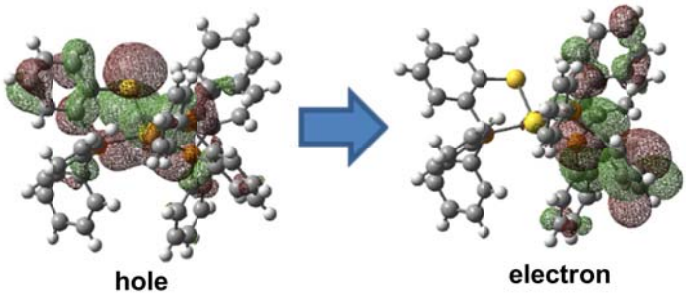

Fig. S12 NTO pairs for the lowest triplet excited state of **3** in X-ray crystal structure.

Table S7 Compositions of hole and electron in the S_1 state of **3**. (X-ray crystal structure)

	percentage composition (%) [a]		
	hole	electron	differences
Au	5.96	0.54	5.42
S	56.4	0.04	56.4
P	4.60	2.77	1.83
P	3.46	1.48	1.98
P	2.35	0.36	1.99
others	27.2	94.8	-67.6

[a] In the molecular orbitals, the atomic component is evaluated by the sum of the square of the LCAO coeffiients which belong to the corresponding atom; see experimental section in detail.

Table S8 Compositions of hole and electron in the T_1 state of **3**. (X-ray crystal structure)

	percentage composition (%) [a]		
	hole	electron	differences
Au	6.20	0.55	5.65
S	55.4	0.05	55.4
P	4.86	2.77	2.09
P	3.82	1.47	2.35
P	2.39	0.37	2.02
others	27.3	94.8	-67.5

[a] In the molecular orbitals, the atomic component is evaluated by the sum of the square of the LCAO coeffiients which belong to the corresponding atom; see experimental section in detail.

hole **electron**

Fig. S13 NTO pairs for the lowest triplet excited state of **1** in optimized S_0 geometry. The generation probabilities are 99.6 %.

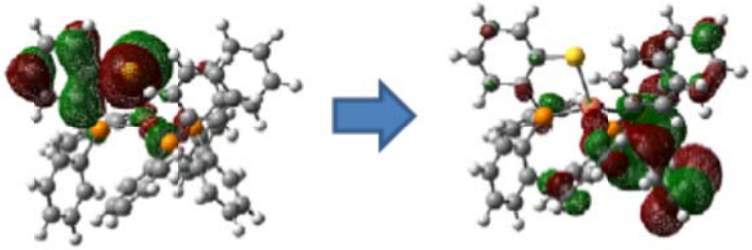

hole **electron**

Fig. S14 NTO pairs for the lowest singlet excited state of **1** in optimized T_1 geometry. The generation probabilities are 99.9 %.

Table S9 Compositions of hole and electron in the T_1 state of **1** (optimized S_0 geometry).

	percentage composition (%) [a]		
	hole	electron	differences
Cu	4.86	0.35	4.51
S	63.3	0.06	63.2
P	2.47	1.44	1.03
P	1.76	3.74	-1.98
P	0.09	0.23	-0.14
others	28.2	94.2	-66.0

[a] In the molecular orbitals, the atomic component is evaluated by the sum of the square of the LCAO coeffiients which belong to the corresponding atom; see experimental section in detail.

Table S10 Compositions of hole and electron in the S_1 state of **1** (optimized T_1 geometry).

	percentage composition (%) [a]		
	hole	electron	differences
Cu	3.20	0.32	2.88
S	62.7	0.04	62.7
P	13.8	1.54	12.3
P	1.02	3.28	-2.26
P	0.25	0.43	-0.18
others	19.0	95.4	-76.4

[a] In the molecular orbitals, the atomic component is evaluated by the sum of the square of the LCAO coeffiients which belong to the corresponding atom; see experimental section in detail.

5. Thermogravimetric Alalysis

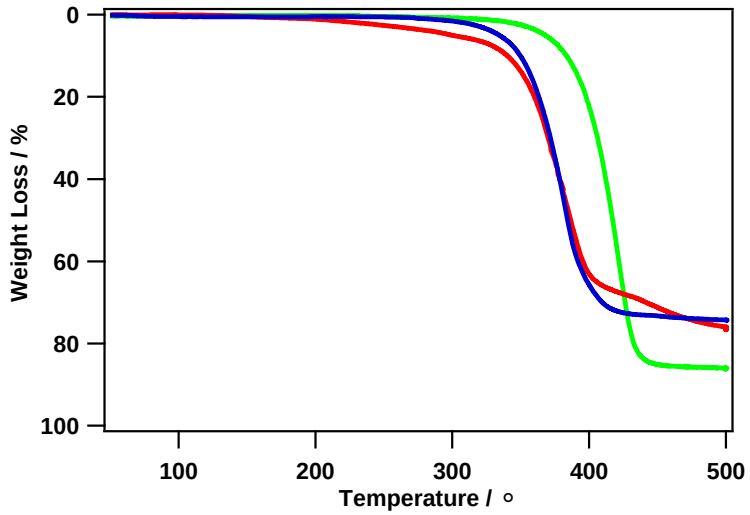

Fig. S15 TGA data for **1** (green), **2** (blue), and **3** (red).

6. Cyclic Voltammetry

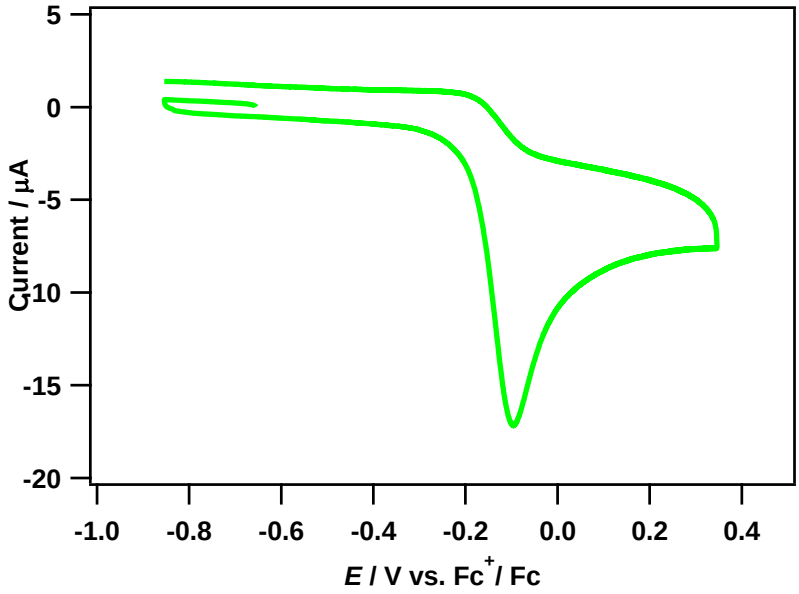

Fig. S16 Cyclic voltammetry of **1**.

7. References

1. E. Block, G. Ofori-Okai and J. Zubieta, J. Am. Chem. Soc., 1989, 111, 2327-2329.
2. A. Tsuboyama, K. Kuge, M. Furugori, S. Okada, M. Hoshino and K. Ueno, *Inorganic Chemistry*, 2007, **46**, 1992-2001.
3. N. Mezailles, L. Ricard and F. Gagosz, *Org. Lett.*, 2005, **7**, 4133-4136.